Contribution of Polar Residues of the J-Helix in the 3′−5′ Exonuclease Activity of *Escherichia coli* DNA Polymerase I (Klenow Fragment): Q677 Regulates the Removal of Terminal Mismatch†

Kamalendra Singh and Mukund J. Modak*

Department of Biochemistry and Molecular Biology, University of Medicine and Dentistry of New Jersey, New Jersey Medical School, Newark, New Jersey 07103

Received January 24, 2005; Revised Manuscript Received April 8, 2005

ABSTRACT: Previous structural and biochemical data indicate a participation of the J-helix of *Escherichia coli* pol I in primer positioning at the polymerase and exonuclease sites. The J-helix contains three polar residues: N675, Q677, and N678. Preliminary characterization of alanine substitutions of these residues showed that only Q677A DNA polymerase has substantially decreased polymerase and increased exonuclease activity. The Q677A enzyme had ∼2- and ∼5-fold greater exonuclease activity than the wild type (WT) with mismatched and matched template−primers (TPs), respectively. N675A and N678A DNA polymerases did not differ significantly from the WT in these activities, despite the fact that both residues are seen to interact with the TP in various pol I−DNA complexes. Pre-steady-state kinetic measurements for the exonuclease activity of WT and mutant enzymes indicated nearly identical DNA binding affinity for ssDNA and mismatched TPs. However, with a matched TP, Q677A DNA polymerase exhibited increased exonuclease site affinity. The most important characteristic of Q677A DNA polymerase was its ability to continue cleavage into the matched region of the TP after mismatch excision, in contrast to the WT and other mutant enzymes. The increase in the exonuclease activity of Q677A DNA polymerase was further determined not to be solely due to the weakened binding at the polymerase site, by comparison with another polymerase-defective mutant enzyme, namely, R668A DNA polymerase. These enzymes have significantly decreased DNA binding affinity at the polymerase site, yet the exonuclease activity parameters of R668A DNA polymerase remain similar to those of the WT. These results strongly suggest that participation of Q677 is required for positioning the primer terminus (a) in the polymerase site for continued nucleotide addition and (b) in the 3′-exonuclease site for the controlled removal of mismatched nucleotides.

DNA polymerases perform faithful DNA replication by an intricate combination of two events: (a) accurate nucleotide incorporation and (b) exonucleolytic removal of an incorrectly added nucleotide. It has been suggested that hydrogen bonding interactions between specific amino acid side chains and the minor groove of the template−primer (TP)[1] play a central role in the ability of a polymerase to distinguish between correct and incorrect base pairs (*1*). In the case of correct base pairs, the positions of two minor groove hydrogen bond acceptors (N3 in purines and O2 in pyrimidines) are topologically similar, but are clearly different in mismatched pairs (*2*). The altered positions of these two atoms (N3 and O2) may perturb the interactions between protein side chains and DNA, which could lead either to steric hindrance or to a loss of hydrogen bonding. This phenomenon may be one of the mechanisms of sensing both paired and mispaired TPs. Thus, the efficient proofreading by polymerase requires the presence of specific side chains within the polymerase domain, which bind the primer strand and also sense mismatched base pairs. Using the Klenow fragment (KF) of *Escherichia coli* DNA polymerase I and T4 DNA polymerase, several attempts have been made to understand the mechanism of "mismatch" sensing in the polymerase site and switching of the primer between the polymerase and exonuclease sites (*3*−*9*).

In an earlier study, we suggested that the conformation of a short segment present in the polymerase domain of KF, namely, the J-helix, influences the partitioning of a primer between these two sites (*9*). Substitution of the C-terminal proline of J-helix with a glycine significantly reduced the polymerase activity but caused an increase in exonuclease activity, indicating a possible role of the J-helix in the coupling of the two activities. These results corroborate the structural data available on the KF as well as other polymerases of the same family (A-family) (*10*−*12*). Thus, in

† Supported in part by a grant from the National Institute of General Medical Sciences (GM 36307).

* To whom correspondence should be addressed: Biochemistry and Molecular Biology, UMD-New Jersey Medical School, 185 South Orange Ave., Newark, NJ 07103. Phone: (973) 972-5515. Fax: (973) 972-5594. E-mail: modak@umdnj.edu.

[1] Abbreviations: pol I, *E. coli* DNA polymerase I; KF, Klenow fragment of *E. coli* DNA polymerase I; DTT, dithiothreitol; BSA, bovine serum albumin; TP, template−primer; KlenTaq, Klenow fragment equivalent of *Thermus aquaticus* DNA polymerase I; Bst, Klenow fragment equivalent of *Bacillus stearothermophilus* DNA polymerase I; ssDNA, single-stranded DNA; dsDNA, double-stranded DNA.

10.1021/bi050140r CCC: $30.25
Published on Web 05/11/2005

Table 1: H-Bonding Interactions of J-Helix Residues As Seen in Different Crystal Structures[a]

structure	interacting atoms	residues involved	distance (Å)	interaction type
apoenzyme	MC−SC	Q677−N675	3.25	intramolecular
	MC−SC	N675−N678	3.94	intramolecular
	SC−SC	N678−N675	3.62	intramolecular
binary (polymerase)	SC−SC	Q677−H881	3.30	intramolecular
(PDB entry 4ktq)	SC−SC	Q677−Q879	3.41	intramolecular
	MC−PO4	P680−primer	3.83	intermolecular
	MC−PO4	I679−primer	3.24	intermolecular
	SC−N3	N678−primer	4.17	intermolecular
	SC−O4′	N675−template	3.36	intermolecular
binary (exonuclease)	SC−PO4	N678−primer	3.42	intermolecular
(PDB entry 1kln)	SC−PO4	N675−primer	3.12	intermolecular

[a] This table shows the inter- and intramolecular hydrogen bonding interactions involving J-helix residues in the apoenzyme (*22*) (PDB entry 1ktq), the polymerase complex (PDB entry 4 ktq) (*12*), and the editing complex (PDB entry 1kln) (*10*). The interactions required for the classical α-helical (between residues *i* and *i* + 4) conformation are not included. The interactions of P680 and I689 equivalent residues with the primer are not hydrogen bonds. Instead, they appear to be of the van der Waals type. MC represents main chain, and SC represents side chain.

the KF−DNA binary complex, with the primer bound to the exonuclease domain, the J-helix conformation as in the apoenzyme is retained, whereas a coiled structure is seen when the TP is bound in the polymerase mode (*11*, *12*).

While biochemical and structural data suggest a role for the J-helix in efficient coordination between polymerase and exonuclease activities, it is not clear whether the alterations in the secondary structure of the J-helix, or the side chain conformation of its three polar residues, are responsible for such coordination. To explore the involvement of these polar side chains in the proofreading activity, we generated alanine mutants of KF at positions N675, Q677, and N678 in an exonuclease positive background. All mutant enzymes together with the WT were biochemically characterized for their polymerase and exonuclease properties, using pre-steady-state kinetic measurements. While all the enzyme species were capable of removing terminal mismatches, Q677A DNA polymerase exhibited an unusual ability to cleave the primer into the matched region of the TP, indicating the loss of recognition of the matched status of the TP. Since Q677 is a member of the H-bonding track formed by five residues (*13*), all of which are required for the polymerase mode binding of the TP, we also examined the properties of another H-bonding track mutant enzyme, R668A. This mutant enzyme clearly lacked the activity to cleave the primer into the matched region of the TP. Our results indicate that despite interaction of N675 and N678 with the TP seen in the crystal structures of DNA bound in the exonuclease or polymerase modes (Table 1), these residues seem to have little or no individual contribution to either polymerase or exonuclease functions. In contrast, Q677, which has no discernible interaction with the TP in reported crystal structures, is required both for binding of the TP in the polymerase mode and for evaluation of the matched status of the TP during removal of terminal mismatch.

EXPERIMENTAL PROCEDURES

Enzymes and Reagents. All mutant enzymes were generated from the plasmid (pCJ141) generously provided by C. Joyce of Yale University (New Haven, CT) (*14*). The maintenance and expression strains for the pCJ141 plasmid, *E. coli* CJ406 and *E. coli* CJ376, respectively, were also obtained from C. Joyce. pfu-turbo polymerase, used for PCR-based site-directed mutagenesis, was from Stratagene. Restriction enzymes and PCR-grade dNTPs were obtained from Roche Molecular Biochemicals. T4 polynucleotide kinase was purchased from Invitrogen Corp. Radiolabeled nucleotides were obtained from PerkinElmer Life Sciences. The DNA extraction kit was from Qiagen, Inc, while DNA oligonucleotides were from MWG Biotechnologies.

In Vitro Site-Directed Mutagenesis, Expression, Purification, and Specific Polymerase Activity of WT and Mutant Proteins. The PCR-based protocol described in Stratagene's QuickChange Site-directed Mutagenesis kit and the pCJ141 plasmid (*14*, *15*) were used to generate the desired mutations of KF. This plasmid contains the *E. coli* KF gene carrying a D424A mutation, which confers deficiency in 3′−5′ exonuclease activity. To generate the WT exonuclease-efficient enzyme, D424A was changed back to D424. The mutant exonuclease-positive mutant DNA polymerases (N675A, Q677A, and N678A) were generated using this reverted (WT) plasmid. All mutations were confirmed by DNA sequencing. Isolation, purification, and determination of specific polymerase activity and steady-state kinetic parameters of N675A, Q677A, N675A, and R668A DNA polymerases were carried out as described previously (*13*).

$K_{D.DNA}$ Determination. DNA binding affinity for ssDNA and TPs containing zero, one, and three mismatches was calculated from the rates of exonucleolytic degradation at different enzyme concentrations (25−150 nM) with 1 nM DNA. The rates of exonuclease activity were plotted against enzyme concentration, and the $K_{D.DNA}$ was determined by fitting the data points to a hyperbola. Here and in subsequent assays, the curve fitting was carried out with either GraphPad Prism or Sigma Plot. The TP binding affinity in the polymerase mode for wild-type, N678A, and N675A DNA polymerases was determined by a gel mobility shift assay as described previously (*13*). Due to the extremely low affinity of Q677A and R668A DNA polymerases, pre-steady-state polymerase kinetics were used to assess TP binding of these two enzymes.

Pre-Steady-State Kinetic Assays of Q677A and R668A Mutant Enzymes. All assays were carried out in 50 mM Tris-HCl (pH 7.5), 50 mM KCl, 5 mM $MgCl_2$, 1 mM DTT, 0.01% BSA, and 10% glycerol at 25 °C by using a Rapid Chemical Quench Flow instrument (KinTek Instruments, University Park, PA). Preincubated KF (80 nM) and DNA (final concentration of 10−160 nM) were loaded into one sample loop, and dGTP (50−100 μM) and $MgCl_2$ (5 mM) were loaded into the other sample loop. Reactions were quenched with 0.3 M EDTA, and the products were analyzed by 16% PAGE in the presence of 8 M urea. The intensities of the bands here, and in all other assays, were quantitated with a PhosphorImager and ImageQuant version 5.2 (Molecular Dynamics). To ensure reproducibility, time courses for each set of DNA and dGTP concentrations were repeated at least two times, and the amplitudes and rate constants that were obtained were in very close agreement.

Data Analysis. The amount of product formed (*P*) was graphed as a function of time (*t*), and the data were fit by

Chart 1

Template-primer used for polymerase activity

49/17-mer
5′-GGAAAATCAGTCACACC-3′
3′-CCTTTTAGTCAGTGTGGAAAATCTCTAGCAGTGGCGCCCGAACAGGGAC-5′

Template-primers used for binary complex formation assay

33/20 + ddC
5′-CGT TAG CCA CTC CGA AGT GCC-3dd′
3′-GCA ATC GGT GAG GCT TCA CGG CAT ATT GCG CGT-5′

21/12 + ddC
5′-CGT TAG CCA CTC C-3dd′
3′-GCA ATC GGT GAG GCT TCA CGG-5′

Matched and mismatched template-primers used for exonuclease assays and in exonuclease/polymerase coupled assay

Single stranded DNAs (14- and 16-mer)
5′-CGT TAG CCA CTC CA-3′
5′-CGT TAG CCA CTC CAG G-3′

33p16/16-mer (matched)
5′-CGT TAG CCA CTC CAG G-3′
3′-GCA ATC GGT GAG GTC CCA CGG CAT ATT GCG CGT-5′

33p16/14-mer (matched)
5′-CGT TAG CCA CTC CA-3′
3′-GCA ATC GGT GAG GTA CCA CGG CAT ATT GCG CGT-5′

33/14-mer (containing one mismatch)
5′-CGT TAG CCA CTC CA-3′
3′-GCA ATC GGT GAG GCT TCA CGG CAT ATT GCG CGT-5′

33/16-mer (containing three mismatches)
5′-CGT TAG CCA CTC CAG G-3′
3′-GCA ATC GGT GAG GCT TCA CGG CAT ATT GCG CGT-5′

nonlinear regression to the burst equation

$$P = A(1 - e^{-kt}) + vt$$

where A is the amplitude of the burst phase, k is the rate constant of the burst phase, and v is the rate of the linear phase. The amplitudes of the burst phases (A) were graphed as a function of total DNA concentration ([DNA]), and the data were fit to the quadratic equation

$$A = 0.5(K_{D.DNA} + [Pol] + [DNA]) - (0.25(K_{D.DNA} + [Pol] + [DNA])^2 - ([Pol][DNA]))^{0.5}$$

where $K_{D.DNA}$ is the dissociation constant for the Pol−DNA complex and [Pol] is the concentration of active polymerase molecules.

Pre-Steady-State Exonuclease Rate Determination. Exonucleolytic cleavage of the labeled primer was observed with ssDNA and matched and mismatched double-stranded TPs (14 or 16 bp region; 0, 1, or 3 mismatches). The 5′-^{32}P-labeled substrates (Chart 1) were 14- or 16-mer single-stranded DNA annealed to the appropriate template to generate matched or mismatched TPs. All reactions were performed at 25 °C in a KinTek rapid quench flow instrument (model RQF-3). The sample in syringe A [containing 1 nM DNA substrate, 0.5 mM EDTA, and 125 nM enzyme in 50 mM Tris-HCl buffer (pH 7.0), 1 mM DTT, and 0.1% BSA] was rapidly mixed with 10 mM $MgCl_2$ in syringe B and the reaction quenched at various times by the addition of EDTA (50 mM, pH 8.0). Because of the extremely slow cleavage rate of the matched TP by KF, the reactions with KF were carried out manually, using the same conditions. The aliquots from the quenched reactions were analyzed on 16% polyacrylamide gels containing 8 M urea.

The exonuclease cleavage rates for ssDNA and the matched TP were determined by using the method initially suggested by Cheng and Kuchta (*16*) and subsequently modified by Konigsberg and colleagues (*17*). In this method, the intensity of each individual degradation product band was multiplied by the number of cuts made to generate that product. The sum of these calculated values was then divided by the total intensity of all bands developed within a given time period. This allowed the exonuclease reaction to be expressed in terms of nucleotides cleaved (for details, see ref *18*). The slope of a plot of nucleotides cleaved versus time then provided the rate of the exonuclease reaction. For mismatch rates, the fraction of primer remaining was plotted against time and the data were fitted to a single-exponential function.

RESULTS

This study was undertaken to clarify the roles of three polar residues of the J-helix in the exonuclease and polymerase functions of *E. coli* DNA polymerase I. Only two of

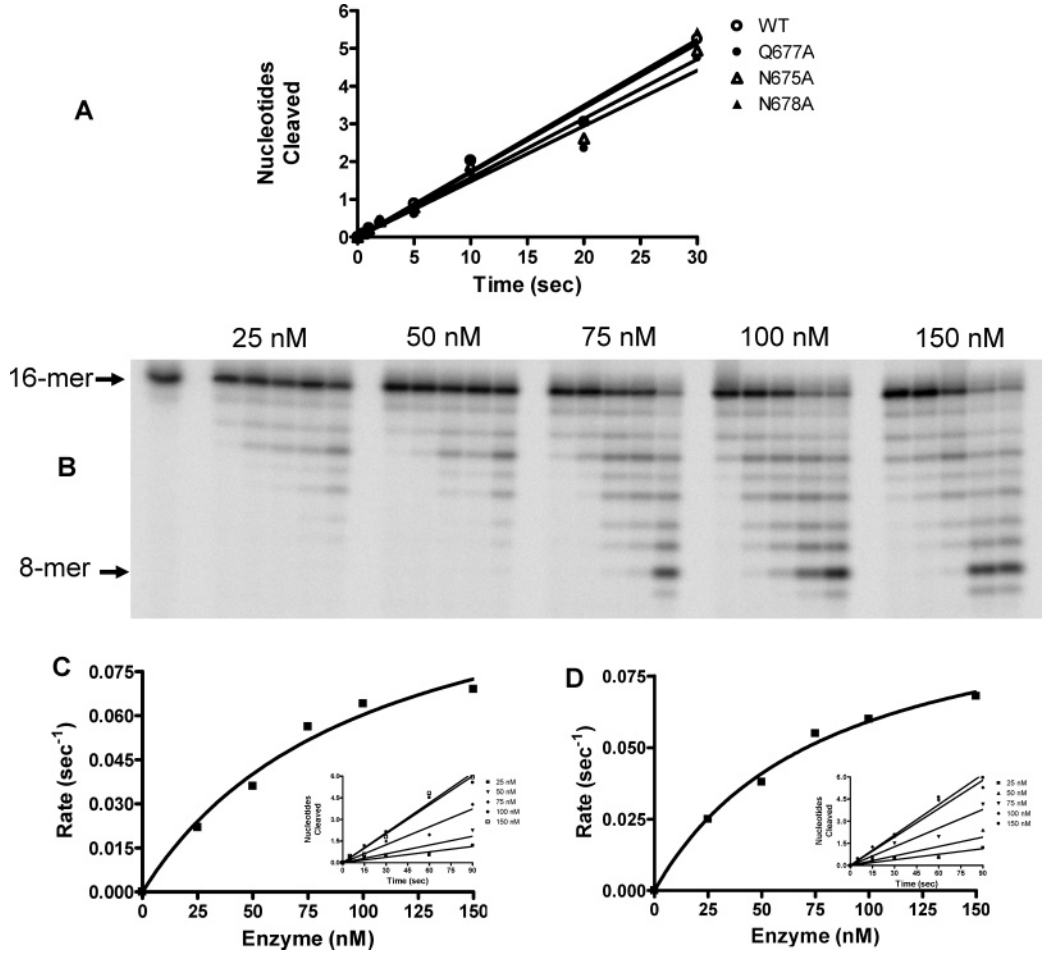

FIGURE 1: 3′−5′ single-stranded DNA binding affinity determination for WT and mutant enzymes using exonuclease activity. The pre-steady-state exonuclease cleavage rates of the WT and mutant enzymes on ssDNA (16-mer) are used to compare relative active site concentrations. The exonuclease activity was assayed by incubating the desired enzyme (125 nM) with various DNA substrates (1 nM DNA), followed by the addition of $MgCl_2$ (5 mM, final concentration) on a rapid quench instrument (KinTek). The DNA binding affinity ($K_{D.DNA}$) in exonuclease mode was determined by plotting the rate of degradation of 1 nM 5′-^{32}P-labeled 16-mer DNA at various enzyme concentrations. Panel B shows the exonuclease degradation profile of the wild-type KF (25−150 nM) at 5, 15, 30, 60, and 90 s. The rate of degradation for each enzyme concentration (shown in the inset in panel C for the WT and in panel D for Q677A) was determined as described in Experimental Procedures. The rates plotted against the enzyme concentration were fitted to a hyperbola to yield the DNA binding affinity.

the three polar residues, namely, N675 and N678, make contacts with the TP in DNA-bound crystal structures, while the third one, Q677, does not have direct interaction, but is required for TP binding in the polymerase mode (*13*). We utilized a combination of pre-steady-state and steady-state kinetic experiments to determine the binding constants of matched and mismatched TPs with wild-type and mutant enzymes so that the contribution of individual residues to the polymerase and exonuclease activities and variations thereof could be discerned.

Steady-State Kinetic Properties of N675A, N678A, and Q677A DNA Polymerases. A steady-state kinetic characterization of mutant enzyme species for polymerase activity clearly showed that Q677A has severely compromised polymerase activity (Table 2), which probably results from its poor TP binding affinity, as judged by the ~60-fold increase in $K_{D.DNA}$, in comparison with that of the wild-type enzyme (*13*). The activity of two other mutant proteins, N675A and N678A, was similar to that of the WT, suggesting that these residues may not be individually required for the polymerase function.

Single-Strand DNA Cleavage Rates, for Comparison of Active Site Concentrations in WT and Individual Mutant Enzymes. Prior to carrying out detailed investigations on exonuclease activity in wild-type and mutant enzymes, we found that the concentrations of active species of enzymes in our preparations needed to be determined so that equal quantities of various enzymes with equal concentrations of active sites could be used. We assumed that the active enzyme species must contain equal active site concentrations for polymerase and exonuclease. Therefore, the titration of either active site would be expected to permit evaluation of the relative concentration of both active sites in each enzyme species. We used the single-stranded DNA degradation property of the WT and mutant enzymes for active site titration. A time course of the exonuclease activity of the WT and three mutant enzymes (125 nM) on ssDNA (1 nM) is shown in Figure 1A. The rates of degradation for WT, Q677A, N675A, and N678A were 0.17, 0.15, 0.16, and 0.17 s^{-1}, respectively. Since the rate of ssDNA degradation under identical conditions of wild-type and mutant enzymes as well as ssDNA binding affinity (as detailed below) is

Table 2: Steady-State Polymerase Kinetic Parameters of Wild-Type KF and Its Mutants[a]

enzyme	$K_{D.DNA}$ (nM)	K_m (μM)	k_{cat} (s^{-1})	k_{cat}/K_m
WT	0.6	5.0	6.0	1.2×10^6
N675A	0.45	9.0	4.0	0.4×10^6
N678A	0.5	7.0	6.0	0.9×10^6
Q677A	41.6	4.0	0.04	0.1×10^5

[a] The steady-state kinetic parameters of $K_{m.dNTP}$ and k_{cat} for the wild-type Klenow fragment and mutants of J-helix residues were measured under conditions where the TP was at a saturating concentration and dNTP was at a variable concentration. Kinetic analysis was performed with a dC_{60}•dG_{18} homopolymer. The $K_{D.DNA}$ determination was carried out as described previously (*13*).

nearly the same, it was inferred that all our enzyme preparations possessed nearly equal "active site" concentrations.

DNA Binding Affinity of WT and Mutant Enzymes in the Exonuclease Mode. Since our earlier studies using steady-state kinetics have shown that P680G mutant KF belonging to the J-helix exhibited increased exonuclease activity (*9*), we evaluated the DNA binding constants for the mutant species of three polar J-helix residues in the exonuclease mode. The pre-steady-state methods were used for these determinations as they provide the rate of activities resulting from a single enzyme DNA encounter. The $K_{D.DNA}$ values for individual enzymes were determined using exonuclease assays with ssDNA and zero-, one-, and three-mismatch-containing TPs. The choice of the substrates is based on the fact that their utilization pattern by the WT enzyme is well-defined. For example, ssDNA and three mismatch-containing TPs predominately bind to the exonuclease site, whereas the matched TP binds to the polymerase site. The TP containing a terminal mismatch is partitioned between both polymerase and exonuclease sites. A representative degradation pattern of ssDNA (1 nM) by the WT (25−125 nM) enzyme is shown in Figure 1B. The rates were calculated from this figure as described by Derbyshire et al. (*18*). The rates of degradation with an increasing enzyme concentration (inset of Figure 1C for the WT and Figure 1D for Q677A DNA polymerase) were fitted to a hyperbola (Figure 1C,D) to determine the $K_{D.DNA}$ at the exonuclease site. There appears to be no significant difference between the WT and mutant proteins with respect to ssDNA binding, as the $K_{D.DNA}$ for all enzymes ranged between 79 and 89 nM. Similarly, the DNA binding affinity for both one- and three-mismatch TPs also did not differ significantly between the WT and mutant enzymes. However, a notable difference was evident in the relative binding of the matched TP with WT and polymerase-defective Q677A mutant enzymes. The $K_{D.DNA}$ values for different substrates for the exonuclease site are collected in Table 3. The $K_{D.DNA}$ for the matched TP in the exonuclease mode for Q677A (~40 nM) was ~2-fold lower than that for the WT (~70 nM) enzyme.

Primer Cleavage Activity of WT and Mutant Enzymes with the Matched TP. Since the activity with the dsDNA substrate with all enzymes is relatively low, the exonuclease activities of WT, N675A, Q677A, and N678A mutant enzymes on the matched TP (33p16/14-mer) were determined using an extended time scale. The rates of exonucleolytic degradation were calculated from plots shown in Figure 2A (data for N675A and N678A are not shown). While the rates for ssDNA degradation were nearly the same for all enzymes (~0.16 s^{-1}) (Table 3), the rates for dsDNA degradation were 0.38, 1.96, 0.55, and 0.59 min^{-1} for WT, Q677A, N675A, and N678A DNA polymerases, respectively.

Primer Cleavage Activity of WT and Mutant Enzymes on a TP Containing One and Three Terminal Mismatches. It has been shown that the rate of removal of the terminal nucleotide is ~2-fold greater with one mismatch at the 3′-end of the primer than with the matched TP (*19*). Recently, using time-resolved fluorescence anisotropy, it has also been shown that DNA mismatch recognition is dependent on specific amino acid residues within the polymerase domain and is not governed solely by thermodynamic differences between correct and mismatched base pairs (*20*). These results suggest that the mismatch is first recognized by binding of the TP into the polymerase active site, followed by its transfer to the exonuclease site. To determine the participation of individual polar residues in this process, we examined the rate of exonucleolytic degradation with mutant enzymes, using one- and three-mismatch-containing TP substrates. The time course of exonucleolytic degradation of a single terminal mismatch by WT and Q677A DNA polymerase is shown in Figure 2B. To calculate the rate of removal of one mismatch, the fraction of 14-mer remaining was plotted against time, and the data points were fitted to a single-exponential decay. The single-mismatch removal rates for WT, Q677A, N678A, and N675A DNA polymerases are provided in Table 3. The rates of mismatch removal by N678A and N675A DNA polymerases were only marginally increased compared to that with the WT. Only the Q677A mutant enzyme exhibited an ~2-fold increase in the exonucleolytic cleavage rate. The exonuclease activity of WT and mutant enzymes on a TP containing three terminal mismatches, at various time points ranging from 0.025 to 1 s, is shown in Figure 2C. The rates of removal of three mismatches are ~3-fold higher than those observed for a single mismatch for all enzymes. As noted for one mismatch, the rate of mismatch removal with three mismatches for Q677A DNA polymerase was ~2-fold greater than that for other enzymes.

It may be pointed out here that our pre-steady-state measurements were carried out in the presence of a 125-fold excess of enzyme over substrate concentration, making it a single-turnover or a single-encounter condition. Nevertheless, because of relatively slow rates of hydrolysis of some substrates (e.g., dsDNA), these products may still have not occurred as a result of a single turnover. To assess this situation, we carried out a trap experiment in which exonuclease activity is monitored after the addition of a 1000-fold excess of unlabeled TP (together with Mg^{2+}) to the preformed enzyme−radiolabeled substrate complex. Results shown in Figure 2D clearly demonstrate that both WT and Q677A DNA polymerases continue cleavage after the addition of the trap. Therefore, our kinetic measurements may be considered to represent a single enzyme−substrate encounter.

Comparative Primer Cleavage Pattern of Activity of Q677A and R668A. Since the Q677A mutant enzyme displayed increased 3′−5′ exonuclease activity with both matched and mismatched TPs but had significantly low polymerase activity, it seemed plausible that other enzymes

Table 3: Exonuclease Activity Parameters of the WT and Mutant Enzymes[a]

		$K_{D.DNA}$ (exonuclease mode) (nM)				exonuclease rate (s^{-1})			
				mismatch				mismatch	
enzyme	$K_{D.DNA}$ (polymerase mode) (nM)	ssDNA	dsDNA	one	three	ssDNA	dsDNA	one	three
WT	0.6 ± 0.2	79 ± 5	70 ± 6	35 ± 4	32 ± 2	0.17 ± 0.02	0.006 ± 0.003	1.53 ± 0.3	4.5 ± 0.9
N675A	0.5 ± 0.1	−	−	34 ± 3	33 ± 4	0.16 ± 0.04	0.009 ± 0.001	1.68 ± 0.2	3.5 ± 0.5
N678A	0.5 ± 0.1	−	−	35 ± 3	27 ± 3	0.17 ± 0.04	0.010 ± 0.001	1.71 ± 0.3	3.8 ± 0.8
Q677A	38 ± 5	88 ± 3	42 ± 2	38 ± 5	32 ± 4	0.15 ± 0.02	0.033 ± 0.008	2.75 ± 0.4	10.2 ± 1.2
R668A	39 ± 4	82 ± 7	37 ± 4	34 ± 4	35 ± 4	0.18 ± 0.02	0.012 ± 0.005	1.61 ± 0.5	3.9 ± 0.6

[a] $K_{D.DNA}$ values for WT, N675A, and N678A enzymes were determined by a gel mobility shift assay as described previously (*13*). Due to the extremely reduced affinity of Q677A and R668A mutant enzymes, the $K_{D.DNA}$ of these enzymes was determined by pre-steady-state polymerase assays as detailed in Experimental Procedures. The DNA binding constants and rates of exonuclease activity with indicated DNA substrates were determined from the results of pre-steady-state kinetics experiments as shown in Figures 1−3.

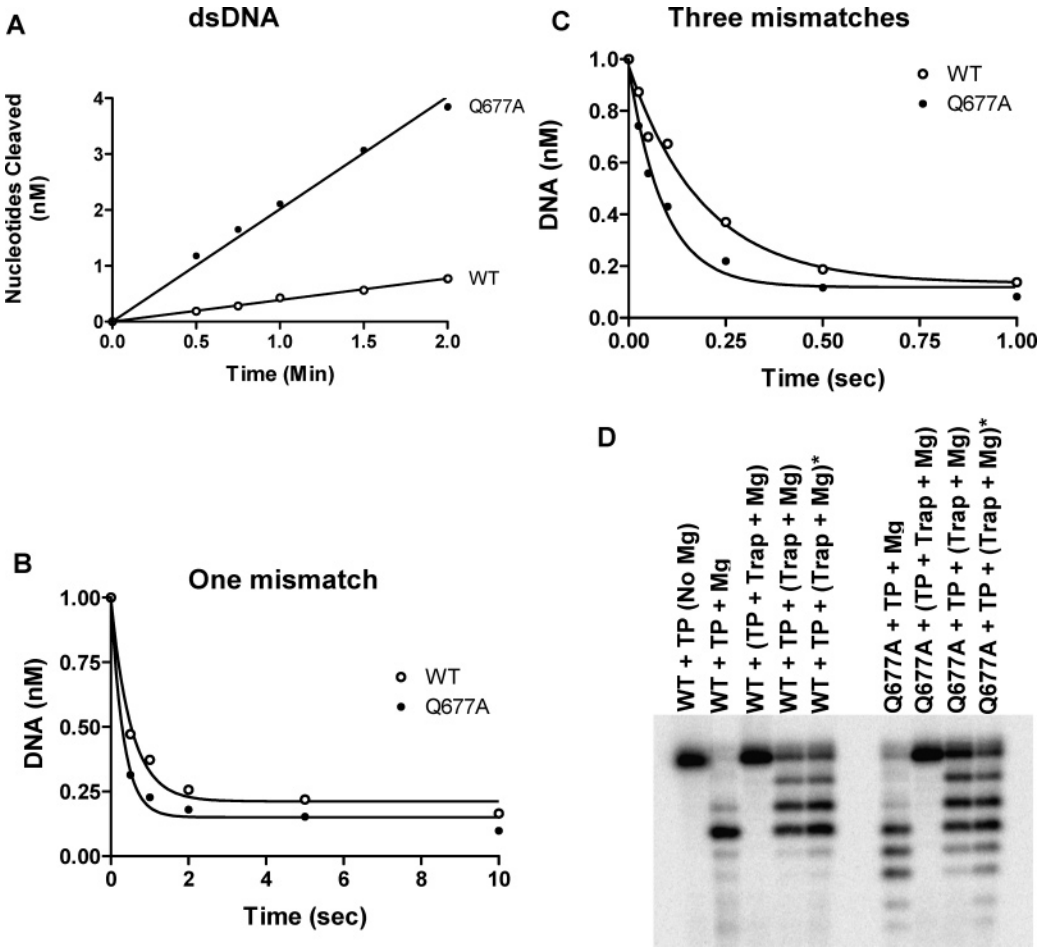

FIGURE 2: Pre-steady-state exonuclease cleavage rates of the WT and mutants on the matched TP (33p16/14), the TP with one mismatch (33/14), and the TP with three mismatches (33/16) in panels A−C, respectively. The exonuclease activity assay conditions were similar to those used for ssDNA shown in Figure 1A, except the reaction time, which varied for TPs containing one and three mismatches (panels B and C, respectively). Reactions with the matched TP were carried out manually since rates of degradation of this substrate are very slow. The reactions were stopped by the addition of 50 mM EDTA at various time intervals. The degradation products were resolved on a 16% polyacrylamide−8 M urea gel. For single-stranded and matched primer degradation, the cleavage rate was determined using the method suggested by Derbyshire et al. (*18*). To determine the rate of cleavage by the WT and mutants on one- and three-mismatch-containing TP, the percent remaining full-length primer was plotted against time and the data were fit to a single-exponential decay using nonlinear regression. The exonuclease activity pattern shown in panel D demonstrates the exonuclease activities of wild-type and Q677A mutant enzymes are operating under single-turnover conditions as judged by the activity in the presence of trap DNA. The reaction mixture contained 125 nM enzyme, 1 nM three-mismatch-containing TP, and 1 μM trap DNA where indicated. The reaction conditions are marked above each lane. The components in parentheses indicate reactions initiated by addition of these components together. The lanes marked with asterisks represent 2 min reactions. All other lanes represent 1 min reactions.

deficient in binding the TP in the polymerase mode would, by default, bind in the exonuclease mode. We therefore examined the properties of an alanine mutant of R668, which was also shown to be defective in binding of the TP in the polymerase mode (*13*). The results of the three-mismatch-containing cleavage activity pattern with R668A DNA polymerase together with that of the WT and Q677A DNA polymerases are shown in Figure 3. As can be seen from this figure, the mismatch portion of the primer is promptly removed by the WT, Q677A, and R668A DNA polymerase;

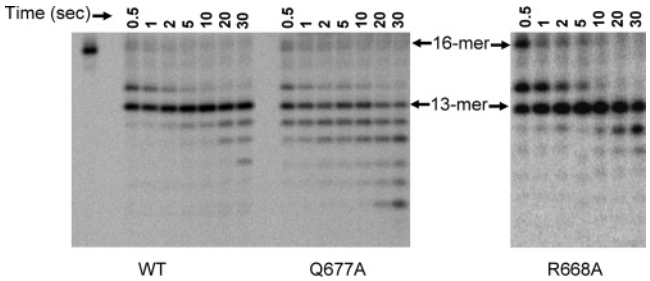

FIGURE 3: Spectrum of exonuclease activity products with three-mismatch-containing TP by WT, Q677A, and R668A mutant enzymes. This figure depicts the continued digestion into the matched portion of the TP (after the mismatch removal) by Q677A but not by the WT and R668A mutant enzymes. The reaction conditions were essentially the same as described in the legend of Figure 2, except that the time points selected for this purpose ranged from 0.5 to 30 s whereas the time interval used for the rate determination of three-mismatch removal (Figure 2C) was from 25 ms to 5 s. The position of the primer is marked as 16-mer and that of matched position as 13-mer.

however, a strong stop in the cleavage activity upon encountering a matched position (shown by the arrow marked 13-mer in Figure 3) is displayed by the WT and R668A mutant enzymes. Similarly, N675A and N678A mutant Klenow fragment enzymes showed a strong stop at the 13-mer position (data not shown). In contrast, Q677A DNA polymerase continued the cleavage of the primer in the matched portion after the removal of the mismatched region. The rate of primer cleavage by Q677A DNA polymerase, into the matched region of the TP (33/13-mer), however, was slow. Nevertheless, the rate of dsDNA degradation after mismatch removal is 0.045 ± 0.005, slightly faster than that observed with dsDNA as an initial substrate (0.033 ± 0.008) (Table 3).

DNA Binding Affinity of Q677A and R668A in the Polymerase Mode. Since both Q677A and R668A are the members of the H-bonding track required for binding of the TP in the polymerase mode (*13*), it seemed plausible that differences in their absolute affinity for the TP in the polymerase mode may be responsible for the variation seen in the exonuclease activity patterns of these mutant species. We therefore carried out pre-steady-state kinetic analysis to determine the DNA binding affinity using a single-nucleotide incorporation assay. These experiments were carried out using a rapid chemical quench flow instrument with 100 nM DNA substrate, 80 nM enzyme, 50 μM dGTP, and 5 mM $MgCl_2$ for times ranging from 1 to 120 s. The kinetics of single-nucleotide incorporation were clearly biphasic for both Q677A and R668A DNA polymerases (panels A and D of Figure 4, respectively), with a rapid burst phase followed by a slow linear phase of nucleotide incorporation. The data were fit to a burst equation with amplitudes of 72 ± 3 and 75 ± 4 nM, respectively, and rate constants equal to 0.21 ± 0.03 and 0.29 ± 0.02 s^{-1} for R668A and Q677A DNA polymerases, respectively, were obtained. The linear rate constants for Q677A and R668A mutant enzymes were equal to 0.0023 ± 0.0005 and 0.0018 ± 0.0003 s^{-1}, respectively.

The amplitude of the pre-steady-state burst phase reflects the concentration of the enzyme−DNA complex at the start of the reaction (*21*). Thus, we could obtain the $K_{D.DNA}$ for DNA binding and the concentration of active enzyme molecules by examining the pre-steady-state kinetics of dGTP incorporation for 1−120 s, using 80 nM enzyme and DNA concentrations ranging from 10 to 160 nM. For each DNA concentration, the amount of 17-mer product formed was graphed as a function of time (Figure 4B,E). The initial time points for each DNA concentration were fit to an exponential equation, using nonlinear regression. The amplitude was then graphed as a function of DNA concentration (Figure 4C,F), and these data were fit using nonlinear regression to a quadratic equation (see Experimental Procedures). This analysis yielded a concentration of active Q677A DNA polymerase equal to 72 ± 2 nM and a $K_{D.DNA}$ for DNA binding equal to 38 ± 5 nM. The concentration of active R668A was 75 ± 2 nM and for DNA binding 39 ± 4 nM. These data suggest that the affinity for the TP was nearly identical for both mutant enzymes. Therefore, the observed difference in the exonuclease rate constants of Q677A and R668A DNA polymerases is not related to the defect in their polymerase mode binding affinities.

DISCUSSION

The analyses of DNA polymerase structures of the pol I family enzymes show that the J-helix region made up of five residues exists in a helical conformation in both the apo-enzyme (*22*, *23*) and DNA bound in exonuclease mode (*10*). However, in the TP-bound structures in polymerase mode (*9*), the J-helix residues are in a coiled conformation. In our previous investigations, we showed that mutation of the C-terminal proline (P680) abolished polymerase activity with exonuclease activity increased compared to that of the WT enzyme (*9*). The J-helix contains three polar residues, namely, N675, Q677, and N678. In different crystal structures, these residues interact differently depending upon the TP binding mode (see Table 1). Thus, in the polymerase mode complex, the side chains of N675 and N678 form hydrogen bonds with the base moieties of the template and/or primer, whereas in the editing complex, they interact with the phosphate backbone of the primer. In contrast, Q677 does not interact with template or primer in either of the complexes. These structural and biochemical data indicate that J-helix residues may control the expression of the polymerase and exonuclease functions of KF. Therefore, to probe the importance of interactions between the TP and KF mediated by individual polar residues of the J-helix, we generated the alanine mutants of N675, Q677, and N678 and investigated the biochemical properties of these mutants.

Most interestingly, of the three mutant enzymes, the polymerase as well as exonuclease activity of N675A and N678A DNA polymerase mutant enzymes was nearly the same as that of the WT, suggesting that these two residues are not essential individually for either activity (Tables 2 and 3). In contrast, significant loss in polymerase and an increase in exonuclease activities were displayed by Q677A DNA polymerase. Earlier, we had shown that Q677 along with R668, H881, Q849, and N845 participates in the formation of the 18 Å long hydrogen bonding track, which facilitates binding of the TP and is required for the polymerase activity (*13*). Pre-steady-state kinetic characterization of the exonuclease activity using ssDNA and zero-, one-, and three-mismatch-containing TPs (Figures 1 and 2) indicated little difference in $K_{D.DNA}$ between WT and mutant enzymes. However, the activity of Q677A DNA polymerase

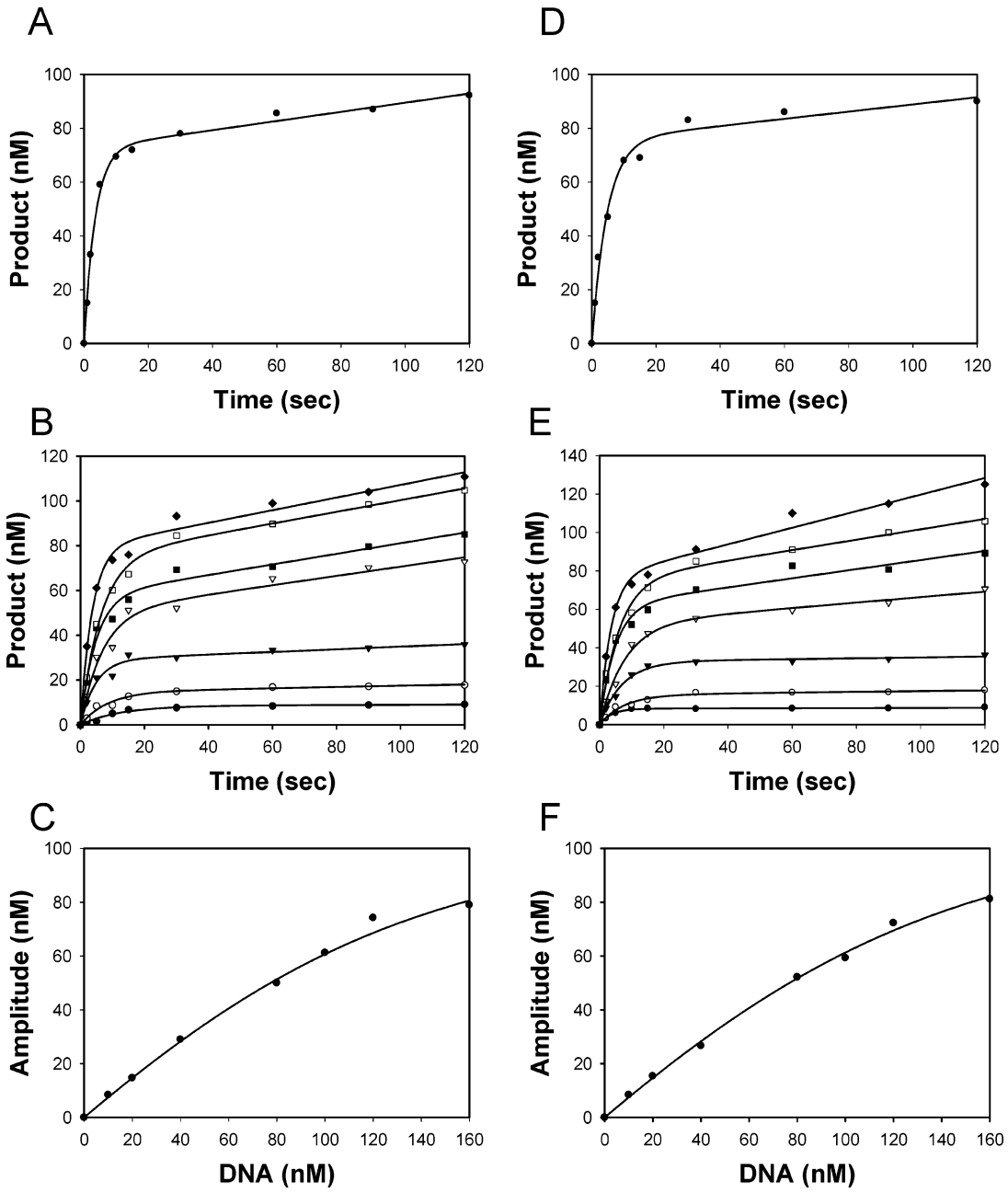

FIGURE 4: Pre-steady-state kinetics of single-nucleotide incorporation by Q677A and R668A mutant enzymes and active site titrations. (A) Q677A (80 nM) and the DNA substrate (100 nM) were mixed with dGTP (100 μM) by using a rapid chemical quench flow instrument for various reaction times. The data were fit to the burst equation with an amplitude of 72 $\pm$ 3 nM and rate constants equal to 0.29 $\pm$ 0.02 and 0.0023 $\pm$ 0.0005 s^{-1}. (B) Q677A (80 nM) and various concentrations of the DNA substrate [(●) 10, (○) 20, (▼) 40, (▽) 80, (■) 100, (□) 120, and (◆) 160 nM] were mixed with dGTP (50 μM) for various reaction times. The solid lines represent the best fits to the burst equation. (C) The amplitudes of the burst phases in panel B (●) were plotted as a function of DNA concentration, and the solid line represents the best fit to the quadratic equation with a $K_{D,DNA}$ for the Q677A−DNA complex equal to 38 $\pm$ 5 nM and an active site concentration equal to 72 $\pm$ 4 nM. (D) R668A (80 nM) and the DNA substrate (100 nM) were mixed with dGTP (100 μM) for various reaction times. The data were fit to the burst equation with an amplitude of 75 $\pm$ 4 nM and rate constants equal to 0.21 $\pm$ 0.03 and 0.0018 $\pm$ 0.0003 s^{-1}. (E) R668A (80 nM) and various concentrations of the DNA substrate [(●) 10, (○) 20, (▼) 40, (▽) 80, (■) 100, (□) 120, and (◆) 160 nM] were mixed with dGTP (50 μM) for various reaction times. The solid lines represent the best fits to the burst equation. (F) The amplitudes of the burst phases in panel E (●) were graphed as a function of DNA concentration, and the solid line represents the best fit to the quadratic equation with a $K_{D,DNA}$ for the R668A−DNA complex equal to 39 $\pm$ 4 nM and an active site concentration equal to 75 $\pm$ 2 nM.

with both matched and mismatched TPs was consistently greater. We, therefore, extensively characterized Q677A DNA polymerase, which exhibited maximal alteration in the catalytic function. The exonuclease activity of Q677A with a perfectly matched TP was ~5-fold greater than that of the WT enzyme. Furthermore, Q677A also cleaves the terminal mismatch ~2 times more efficiently (Table 3). These observations suggest that Q677 of the J-helix is a primary contributor in control of exonuclease activity and that the observed increase in the rate of exonuclease activity of its mutant phenotype, Q677A DNA polymerase, is probably the result of its decreased dissociation from the substrates.

The visual examination of the exonuclease reaction products with three mismatch-containing TPs by the WT and

three mutant enzymes was quite revealing with respect to the cleavage products (Figure 3). WT, N675A, and N678A DNA polymerases stall after the removal of terminal mismatch, i.e., after the generation of matched template-primer
(33/13-mer), as evidenced by the accumulation of 13-mer product (Figure 3). Such a stalling was significantly less evident with the Q677A mutant enzyme, which continues to cleave in the paired region of the TP, although the rate of cleavage in the double-stranded region is slower. The generation of a 13-mer as the major product by WT (as well as by N675A and N678A DNA polymerases) suggests that once the mismatch is removed, the enzyme has a mechanism for sensing the base-pairing nature of the TP and arrests its further degradation most likely by shifting it to the polymerase site. The Q677A DNA polymerase enzyme clearly lacked this activity. However, one possible argument against this scenario may be that all mutant enzymes which exhibit loss of binding in the polymerase mode may have intrinsic ability to continue the degradation of the primer in the matched region of the TP. We therefore compared the properties of another polymerase defective mutant enzyme, namely, R668A. The loss of polymerase activity in this mutant enzyme, similar to that of Q677A, was shown to be due to significantly weakened TP binding in the polymerase mode (*13*). The detailed investigation of the exonuclease properties of R668A by means of pre-steady-state kinetic parameters indicated that its DNA binding constants for ssDNA, dsDNA, and mismatched DNA substrates were similar to those of the WT enzyme (Table 3). The studies on partitioning of the TP by KF and some of its mutant derivatives by Millar and colleagues (*20*), using fluorescence probe-labeled TPs, have also shown that several polymerase defective mutant enzymes exhibited very similar binding constants at the exonuclease site. Interestingly, $K_{D.DNA.exo}$ values determined by fluorescence method for the wild-type and R668A mutant (*20*, *24*) are in close agreement with those determined by pre-steady-state exonuclease activity measurements (Table 3). However, a possibility remained that the decreased TP binding affinity of Q677A DNA polymerases at the polymerase site may be responsible for the difference in the exonuclease properties of this enzyme. We therefore compared the pre-steady-state kinetic parameters for the polymerase reaction catalyzed by Q677A with those of R668A DNA polymerase. The results showed nearly identical binding affinities for the TP in the polymerase mode by Q677A and R668A DNA polymerases (Figure 4 and Table 3). The $K_{D.DNA}$ for the two mutant enzymes was 37−39 nM, significantly greater than that of the WT enzyme (∼0.6 nM). These results clearly indicate that binding of the TP at the polymerase site in both Q677A and R668A mutant enzymes is equally weakened and is not the sole reason for the increased exonuclease activity seen with only the Q677A enzyme. The pre-steady-state analyses for determining the binding affinity for mismatched and matched TP in the exonuclease mode have also revealed that Q677A and R668A mutant DNA polymerases have very similar binding constants. However, the rate of mismatch removal by the R668A enzyme was lower than that of Q677A and was similar to that of the WT enzyme. It is possible that despite very similar $K_{D.DNA}$ rates for the exonuclease reaction, the on and off rates may differ for the two mutant enzymes. Regardless of the actual mechanism, the participation of Q677 in the regulation of two activities (polymerase and exonuclease) appears to be certain. On the basis of our observations, it is clear that the Q677-containing enzyme (i.e., WT) has a better ability to recognize a matched versus a mismatched primer end, which is lost by the Q677A substitution. However, alternative roles for Q677 have not been ruled out. For example, failure to shuttle primer, after mismatch removal, to the polymerase site could very well explain the continued cleavage into the matched region by the Q677A enzyme. Another possibility is that Q677 participates in translocation of pol I after nucleotide incorporation. Its mutation (Q677A) would therefore cause a failure to translocate to the next template nucleotide, triggering another cycle of proofreading. These possibilities need to be resolved to pinpoint the contributions of Q677 to the mechanisms of polymerase and nuclease activities. In any event, the weakened ability of Q677A DNA polymerase to dissociate from the exonuclease site and its significantly weakened binding affinity for the matched TP at the polymerase site definitely implicate Q677 as an essential residue required for appropriate functioning of both polymerase and exonuclease activities. This is perhaps the first residue in the pol I family of enzymes that is shown to be essential for the functioning of both polymerase and proofreading activities.

ACKNOWLEDGMENT

We thank Dr. Smita Patel and Dr. Rajiv Bandwar for many useful discussions and providing us access to the instrumentation facility to perform pre-steady-state kinetic analysis. We also thank Dr. Harold Calvin for editorial assistance.

REFERENCES

1. Seeman, N. C., Rosenberg, J. M., and Rich, A. (1976) Sequence-specific recognition of double helical nucleic acids by proteins, *Proc. Natl. Acad. Sci. U.S.A. 73*, 804−808.
2. Brown, T., and Kennard, O. (1992) Structural basis of DNA mutagenesis, *Curr. Biol. 2*, 299.
3. Joyce, C. M. (1989) How DNA travels between the separate polymerase and 3′−5′-exonuclease sites of DNA polymerase I (Klenow fragment), *J. Biol. Chem. 264*, 10858−10866.
4. Spacciapoli, P., and Nossal, N. G. (1994) A single mutation in bacteriophage T4 DNA polymerase (A737V, tsL141) decreases its processivity as a polymerase and increases its processivity as a 3′→5′ exonuclease, *J. Biol. Chem. 269*, 438−446.
5. Stocki, S. A., Nonay, R. L., and Reha-Krantz, L. J. (1995) Dynamics of bacteriophage T4 DNA polymerase function: Identification of amino acid residues that affect switching between polymerase and 3′ → 5′ exonuclease activities, *J. Mol. Biol. 254*, 15−28.
6. Baker, R. P., and Reha-Krantz, L. J. (1998) Identification of a transient excision intermediate at the crossroads between DNA polymerase extension and proofreading pathways, *Proc. Natl. Acad. Sci. U.S.A. 95*, 3507−3512.
7. Reha-Krantz, L. J. (1998) Regulation of DNA polymerase exonucleolytic proofreading activity: Studies of bacteriophage T4 "antimutator" DNA polymerases, *Genetics 148*, 1551−1557.
8. Reha-Krantz, L. J., Marquez, L. A., Elisseeva, E., Baker, R. P., Bloom, L. B., Dunford, H. B., and Goodman, M. F. (1998) The proofreading pathway of bacteriophage T4 DNA polymerase, *J. Biol. Chem. 273*, 22969−22976.
9. Tuske, S., Singh, K., Kaushik, N., and Modak, M. J. (2000) The J-helix of *Escherichia coli* DNA polymerase I (Klenow fragment) regulates polymerase and 3′−5′-exonuclease functions, *J. Biol. Chem. 275*, 23759−23768.
10. Beese, L. S., Derbyshire, V., and Steitz, T. A. (1993) Structure of DNA polymerase I Klenow fragment bound to duplex DNA, *Science 260*, 352−355.

11. Doublie, S., Tabor, S., Long, A. M., Richardson, C. C., and Ellenberger, T. (1998) Crystal structure of a bacteriophage T7 DNA replication complex at 2.2 Å resolution, *Nature 391*, 251−258.
12. Li, Y., Korolev, S., and Waksman, G. (1998) Crystal structures of open and closed forms of binary and ternary complexes of the large fragment of *Thermus aquaticus* DNA polymerase I: Structural basis for nucleotide incorporation, *EMBO J. 17*, 7514−7525.
13. Singh, K., and Modak, M. J. (2003) Presence of 18-Å long hydrogen bond track in the active site of *Escherichia coli* DNA polymerase I (Klenow fragment). Its requirement in the stabilization of enzyme-template-primer complex, *J. Biol. Chem. 278*, 11289−11302.
14. Polesky, A. H., Steitz, T. A., Grindley, N. D., and Joyce, C. M. (1990) Identification of residues critical for the polymerase activity of the Klenow fragment of DNA polymerase I from *Escherichia coli*, *J. Biol. Chem. 265*, 14579−14591.
15. Polesky, A. H., Dahlberg, M. E., Benkovic, S. J., Grindley, N. D., and Joyce, C. M. (1992) Side chains involved in catalysis of the polymerase reaction of DNA polymerase I from *Escherichia coli*, *J. Biol. Chem. 267*, 8417−8428.
16. Cheng, C. H., and Kuchta, R. D. (1993) DNA polymerase ϵ: Aphidicolin inhibition and the relationship between polymerase and exonuclease activity, *Biochemistry 32*, 8568−8574.
17. Lin, T. C., Karam, G., and Konigsberg, W. H. (1994) Isolation, characterization, and kinetic properties of truncated forms of T4 DNA polymerase that exhibit 3′−5′ exonuclease activity, *J. Biol. Chem. 269*, 19286−19294.
18. Derbyshire, V., Pinsonneault, J. K., and Joyce, C. M. (1995) Structure−function analysis of 3′→5′-exonuclease of DNA polymerases, *Methods Enzymol. 262*, 363−385.
19. Kuchta, R. D., Benkovic, P., and Benkovic, S. J. (1988) Kinetic mechanism whereby DNA polymerase I (Klenow) replicates DNA with high fidelity, *Biochemistry 27*, 6716−6725.
20. Thompson, E. H., Bailey, M. F., van der Schans, E. J., Joyce, C. M., and Millar, D. P. (2002) Determinants of DNA mismatch recognition within the polymerase domain of the Klenow fragment, *Biochemistry 41*, 713−722.
21. Johnson, K. A. (1998) Advances in transient-state kinetics, *Curr. Opin. Biotechnol. 9*, 87−89.
22. Korolev, S., Nayal, M., Barnes, W. M., Di Cera, E., and Waksman, G. (1995) Crystal structure of the large fragment of *Thermus aquaticus* DNA polymerase I at 2.5-Å resolution: Structural basis for thermostability, *Proc. Natl. Acad. Sci. U.S.A. 92*, 9264−9268.
23. Kiefer, J. R., Mao, C., Hansen, C. J., Basehore, S. L., Hogrefe, H. H., Braman, J. C., and Beese, L. S. (1997) Crystal structure of a thermostable *Bacillus* DNA polymerase I large fragment at 2.1 Å resolution, *Structure 5*, 95−108.
24. Carver, T. E., Jr., Hochstrasser, R. A., and Millar, D. P. (1994) Proofreading DNA: Recognition of aberrant DNA termini by the Klenow fragment of DNA polymerase I, *Proc. Natl. Acad. Sci. U.S.A. 91*, 10670−10674.

BI050140R